Carbonic Anhydrase Inhibitors: Bioreductive Nitro-Containing Sulfonamides with Selectivity for Targeting the Tumor Associated Isoforms IX and XII[▽]

Katia D'Ambrosio,[†,‡] Rosa-Maria Vitale,[†,§] Jean-Michel Dogné,[||] Bernard Masereel,[||] Alessio Innocenti,[⊥] Andrea Scozzafava,[⊥] Giuseppina De Simone,*[,‡] and Claudiu T. Supuran*[,⊥]

Istituto di Biostrutture e Bioimmagini-CNR, via Mezzocannone 16, 80134 Napoli, Italy, Istituto di Chimica e Biomolecolare-CNR, via Campi Flegrei 34, 80078, Pozzuoli, Italy, Drug Design and Discovery Center, University of Namur, 61 rue de Bruxelles, 5000 Namur, Belgium, Università degli Studi di Firenze, Laboratorio di Chimica Bioinorganica, Rm. 188, Via della Lastruccia 3, I-50019 Sesto Fiorentino (Firenze), Italy

Received February 5, 2008

2-Substituted-5-nitro-benzenesulfonamides incorporating a large variety of secondary/tertiary amines were explored as inhibitors of the zinc enzyme carbonic anhydrase (CA, EC 4.2.1.1), with the aim of designing bioreductive inhibitors targeting the hypoxia overexpressed, tumor-associated isozymes. The compounds were ineffective inhibitors of the cytosolic isoform I, showed a better inhibition of the physiologically relevant CA II (K_Is of 8.8−4975 nM), and strongly inhibited the tumor-associated CA IX and XII (K_Is of 5.4−653 nM). Some of these compounds showed excellent selectivity ratios for the inhibition of the tumor-associated isozymes over the cytosolic ones (in the range of 10−1395). The X-ray crystal structure of the adduct of hCA II with the lead molecule 2-chloro-5-nitro-benzenesulfonamide as well as molecular modeling studies for interaction with hCA IX afforded a better understanding of factors governing the discrimination of the two isoforms for this type of bioreductive compound targeting specifically hypoxic tumors.

Introduction

Carbonic anhydrase (CA, EC 4.2.1.1), the catalyst for the interconversion between carbon dioxide and bicarbonate, is an essential enzyme all over the phylogenetic tree, being present in *Bacteria*, *Archaea*, and *Eukaryotes*.[1,2] In humans, the CA-catalyzed reaction is involved in respiration and transport of CO_2/bicarbonate between metabolizing tissues and lungs, pH and CO_2 homeostasis (as a proton is also generated during the catalytic turnover), electrolyte secretion in a variety of tissues/organs, biosynthetic reactions (such as gluconeogenesis, lipogenesis and ureagenesis), bone resorption, tumorigenicity, and many other physiological and pathological processes.[1,2] Many of the CA isozymes involved in these processes, among the 15 known in humans, are important therapeutic targets with the potential to be inhibited or activated to treat a wide range of disorders.[1,2] The main class of CA inhibitors (CAIs) is constituted by substituted benzene sulfonamides and their bioisosteres (sulfamates, sulfamides, etc.), which bind to the Zn^{2+} ion of the enzyme, by substituting the nonprotein zinc ligand to generate a tetrahedral adduct and participating in various other favorable interactions with amino acid residues situated in the active site.[1,2] Several such agents are clinically used drugs, such as acetazolamide **AZA**, methazolamide **MZA**, ethoxzolamide **EZA**, sulthiame **SLT**, dichlorophenamide **DCP**, dorzolamide **DZA**, brinzolamide **BRZ**, and indisulam **IND**.[1,2] A critical problem in the design of CAIs is related to the high number of isoforms, their rather diffuse localization in many tissues/organs, and the lack of isozyme selectivity of the presently available inhibitors.[1,2]

Hypoxia, a condition associated with many types of cancers, triggers a strong overexpression of at least two CA isozymes, i.e., CA IX and XII.[3,4] CA IX belongs to the very active human CAs, its catalytic properties for the CO_2 hydration reaction being comparable with those of the highly evolved catalyst CA II, whereas CA XII is slightly less effective.[1−4] Like all mammalian CAs, CA IX and XII are susceptible to inhibition by sulfonamides/sulfamates/sulfamides and the inorganic atheir anions.[5−7] The almost exclusive localization of CA IX (and to a less degree of CA XII) in tumors make these protein isoforms attractive targets for the design of conceptually novel antitumor therapies.[1−4] In a preceding work we reported hypoxia-activatable sulfonamides incorporating disulfide functionalities.[7] Here we extend the earlier work to sulfonamides incorporating nitro moieties, and we report the inhibitory activity of a series of such aromatic derivatives against the physiologically relevant isoforms I, II, and the tumor-associated ones CA IX and XII. X-ray crystallography and molecular modeling was also employed for rationalizing some of our results.

Results and Discussion

Chemistry and CA Inhibition Studies. Nitroaromatics and the structurally related N-oxides constitute an important class of therapeutic agents against a variety of protozoan and bacterial infections of humans and animals,[8] as well as prodrugs (bioreductive agents), useful for the treatment or imaging of hypoxic tumors.[8−13] Metronidazole **MND** is a well-known and widely clinically used representative of the first type of such compounds,[8] whereas pimonidazole **PIMO**, misonidazole **MISO** (and its ^{18}F-labeled derivative), and tirapazamine **TRPA** are molecular bioimaging markers or bioreductive agents (**TRPA**) useful for the diagnosis and treatment of hypoxic tumors.[9−13] In all of them, the presence of the bioreducible NO_2/NO moieties is critical for the diagnostic/therapeutic properties of these agents. Considering that the CA isozymes IX and XII

* To whom correspondence should be addressed. Phone: +39-081-2534579 (G.D.S.); +39-055-4573005. (C.T.S.). Fax: +39-081-2536642 (G.D.S.); +39-055-4573385 (C.T.S.). E-mail: gdesimon@unina.it (G.D.S.); claudiu.supuran@unifi.it (C.T.S.).

[▽] Coordinates and structure factors have been deposited in the Brookhaven Protein Data Bank (accession code 2QP6).

[†] These authors made equal contributions to this work.
[‡] Istituto di Biostrutture e Bioimmagini-CNR.
[§] Istituto di Chimica e Biomolecolare-CNR.
[||] Drug Design and Discovery Center, University of Namur.
[⊥] Università degli Studi di Firenze, Laboratorio di Chimica Bioinorganica.

10.1021/jm800121c CCC: $40.75
Published on Web 05/16/2008

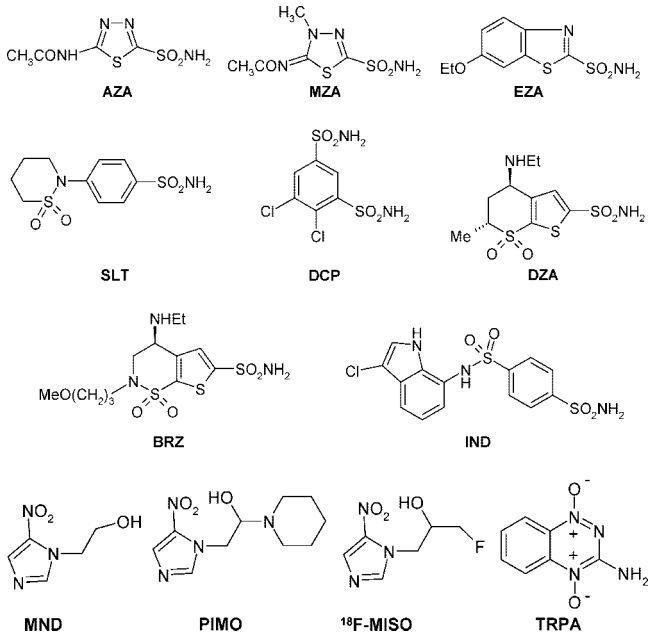

Scheme 1. Reduction/Bioreduction of a Nitro-Benzenesulfonamide (**1**) to the Corresponding Aniline (**2**) or of a Disulfide-Containing Sulfonamide (**3**) to the Corresponding Thiol **4**

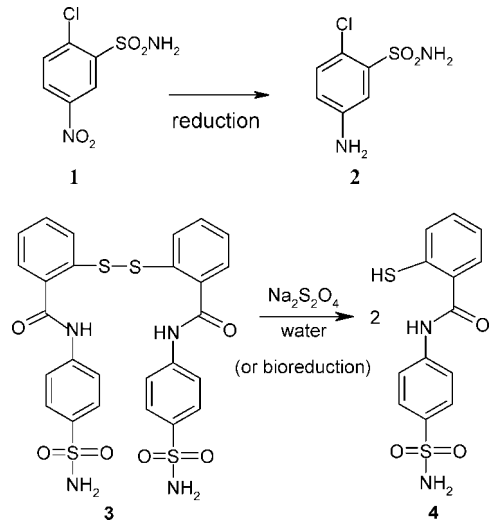

are also highly overexpressed in hypoxic tumors,[1–4] as mentioned above, we explore here the possibility of designing bioreductive CA IX/XII inhibitors incorporating such nitro-aromatic moieties. For this purpose, we first considered a very simple model compound, namely 2-chloro-5-nitrobenzene-sulfonamide **1**, which may be reduced (chemically or enzymatically) to the corresponding amino-sulfonamide **2** (Scheme 1). We observed that both **1** and especially **2** act as potent and rather selective inhibitors of CA IX (see discussion later in the text and Table 1). Thus, we envisaged the possible use of such derivatives as bioreductive, hypoxic tumor-selective agents, similarly to the sulfonamide disulfides **3** (which are reduced to the thiols **4**), investigated earlier by our group (Scheme 1).[7]

Thus, considering **1** as lead molecule, a library of previously reported[14] 2-substituted-5-nitro-benzenesulfonamides (intermediates used for obtaining thromboxane receptor antagonists)[14] of types **A1**−**A20** and **B1**−**B3** was investigated for the inhibition of four physiologically relevant CA isozymes, i.e., the cytosolic, house-keeping CA I and II, as well as the transmembrane, tumor-associated CA IX and XII (Table 1). The main feature of these derivatives is that the 2-substituted-5-nitrobenzenesulfonamide scaffold present in the lead **1** was maintained, with the main distinction being that **A1**−**A20** have secondary amines in ortho to the sulfamoyl moiety, whereas derivatives **B1**−**B3** possess tertiary amines in this position. These ortho substituents incorporate aliphatic, linear chain, or cyclic moieties (**A1**−**A6**) as well as aromatic (**A7**−**A20**) or heterocylic (**B1**−**B3**) amines. The nature of these groups was chosen in such a way as to provide a wide insight in SAR for this class of compounds.

Table 1. Inhibition Data of Sulfonamides **1**−**4**, **A1**−**A20**, and **B1**−**B3** Investigated in the Present Paper and Standard CA Inhibitors (**AZA**−**IND**), against CA Isozymes I, II (cytosolic), IX, and XII (Transmembrane), by a Stopped-Flow, CO_2 Hydration Assay[15]

		K_I[b]		
inhibitor	hCA I[a] (μM)	hCA II[a] (nM)	hCA IX[c] (nM)	hCA XII[c] (nM)
AZA	0.25	12	25	5.7
MZA	0.050	14	27	3.4
EZA	0.025	8	34	22
DCP	1.20	38	50	50
DZA	50	9	52	3.5
BRZ	45	3	37	3.0
IND	0.031	15	24	3.4
1	0.21	208	75	17.9
2	6.2	58.9	38.2	10.5
3[d]	4.35	4975	653	nt[e]
4[d]	0.27	16	9.1	nt[e]
A1	3.1	86	11.8	7.3
A2	11.6	112	10.5	12.3
A3	7.0	74.6	10.8	9.5
A4	12.7	80	9.6	9.1
A5	3.1	82	85	74
A6	8.8	430	273	246
A7	0.10	106	11.4	10.3
A8	1.8	38.5	10.6	9.0
A9	5.4	61	11.2	9.8
A10	0.10	73.7	10.3	7.5
A11	6.3	100	14.0	11.5
A12	3.1	52.3	33.4	28.2
A13	7.8	35.3	8.4	7.5
A14	8.2	8.8	9.3	6.5
A15	4.2	40.4	38.8	27.1
A16	10.9	506	289	175
A17	10.3	50.4	7.4	11.8
A18	12.6	44.5	11.6	13.5
A19	9.8	9.3	11.5	10.1
A20	3.6	98	7.9	5.8
B1	3.5	50.1	12.5	10.4
B2	7.5	9.0	9.5	6.1
B3	7.4	116	93	79

[a] Human, recombinant isozymes. [b] Errors in the range of 5−10% of the shown data, from three different assays, by a CO_2 hydration stopped-flow assay.[15] [c] Catalytic domain of human, cloned isoform.[12,13] [d] From ref 7. [e] nt = not tested.

The analysis of inhibition data presented in Table 1 reveals that against the slow cytosolic isozyme hCA I, the compounds **1, 2**, **A1**−**A20**, and **B1**−**B3** investigated here behaved as medium potency inhibitors, with inhibition constants in the range of 0.10−12.7 μM. It may be observed that the best CA I inhibitors (submicromolar activity, i.e., K_Is of 0.10−027 μM) were **1**, **A7**, and **A10**. Thus, the lead molecule **1** shows affinity for this isozyme in the same range as the clinically used drug acetazolamide, **AZA**, or the thiol-sulfonamide **4** investigated earlier.[7] The introduction of the phenylamino- (**A7**) or *p*-tolylamino (**A10**) moieties in ortho to the sulfamoyl group leads to a slightly better inhibition profile of these two derivatives over the lead **1** (K_Is of 0.10 μM for **A7** and **A10** versus 0.21 μM of **1**, respectively), whereas all other substitution patterns present in the remaining derivatives led to a diminished

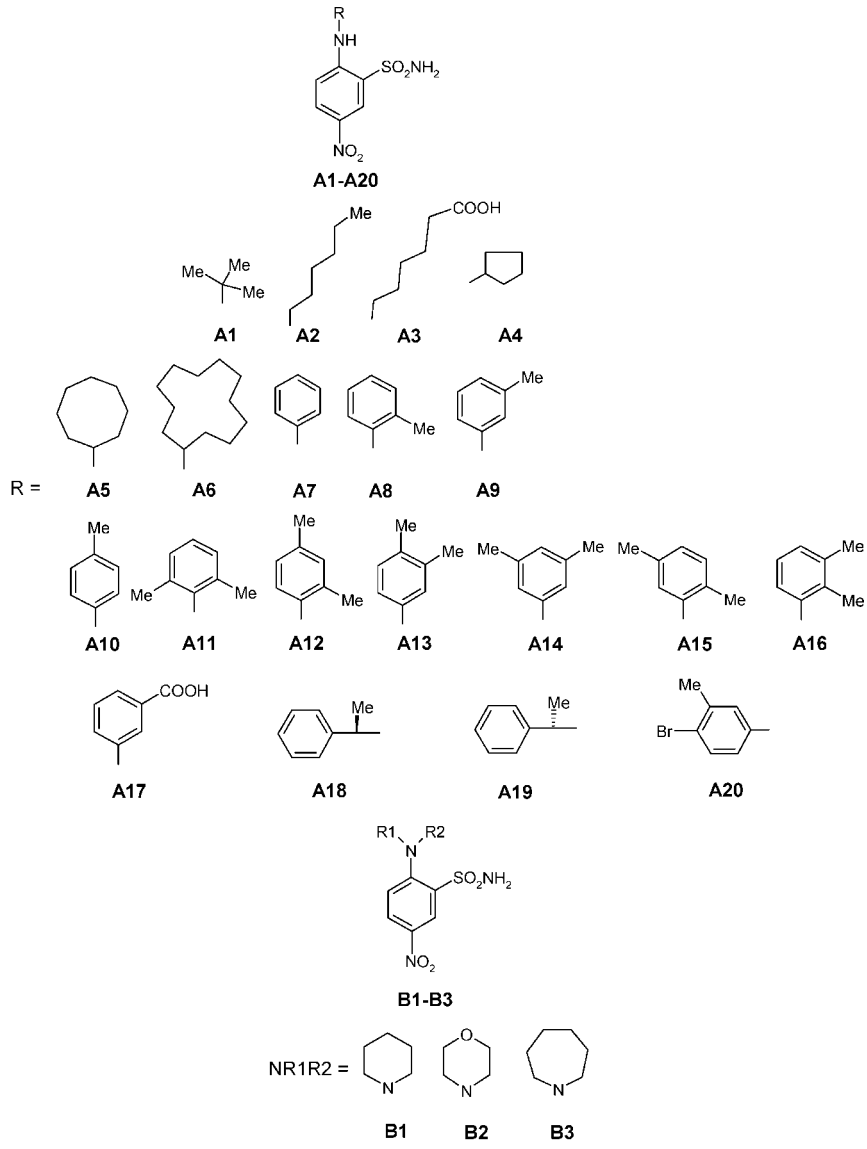

inhibitory power of the corresponding sulfonamides as compared to the lead **1** (Table 1). Most of these derivatives (including **2**, **A1**, **A3**, **A5**, **A6**, **A8**, **A9**, **A11**−**A15**, **A20**, and **B1**−**B3**) showed a rather flat SAR, with K_Is varying not very much, in the range of 1.8−8.8 μM. These findings demonstrated that both aliphatic amines or aromatic monosubstituted (in ortho and meta) or disubstituted amines are equally ineffective for obtaining strong CA I inhibitors belonging to this class of sulfonamides. The compounds with the lowest affinity for CA I were **A2**, **A4**, and **A16**−**A19**, which showed K_Is in the range of 9.8−12.7 μM. Again, two of these derivatives incorporate aliphatic (acyclic or cyclic) amine moieties in ortho to the sulfamoyl group (**A2** and **A4**), whereas the remaining ones are aromatic or aralkylamines (**A16**−**A19**).

It should be also noted that the simple amino-derivative **2** is a 29.5 times weaker CA I inhibitor as compared to the corresponding nitroderivative **1**. This is probably due to the uncompensated acidifying effect of the nitro group on the sulfonamide moiety because most CAIs bind in deprotonated form, as RSO_2NH^- anions, to the Zn^{2+} ion within the enzyme active site.[1–7]

Against the dominant, physiologically highly relevant isoform hCA II,[1] the sulfonamides investigated here showed a very different behavior as compared to what discussed above for hCA I. Thus, most of these compounds showed good inhibitory power, with K_Is in the range of 8.8−506 nM. The best inhibitors were **A14**, **A19**, and **B2**, which with K_Is of 8.8−9.3 nM showed the same potency as the clinically used derivatives **AZA**, **MZA**, **EZA**, **DRZ**, or **IND** (Table 1). Other derivatives, such as **2**, **A1**, **A3**−**A5**, **A8**−**A10**, **A12**, **A13**, **A15**, **A17**, **A18**, **A20**, and **B1**, showed a weaker CA II inhibitory capacity, with K_Is in the range of 35.3−98 nM, with most of these compounds showing the same type of activity against CA II as the clinically used drug dichlorophenamide **DCP** (Table 1).[1,19] They incorporate both secondary and tertiary amines functionalized with both aliphatic and aromatic groups, similarly to what was mentioned above for the inhibition of CA I. A last group of sulfonamides, i.e., **1**, **A2**, **A6**, **A7**, **A11**, **A16**, and **B3**, showed a weaker CA II inhibitory capacity as compared to the compounds discussed above, with K_Is in the range of 100−506 nM (Table 1). From the analysis of these data, it may be observed that even very small alterations in the structure of these compounds lead to a drastic change in the CA II inhibitory capacity. For example the replacement of an oxygen atom in **B2** by a corresponding CH_2 group in **B1** leads to a 5.5 times worse CA II inhibitor. Furthermore, an additional CH_2 moiety, as in **B3**, is even more detrimental to the biological activity, the compound being an inhibitor 12.8 times less effective as compared to **B2** and a 2.3

times as compared to **B1**. Another example is offered by **A14** and **A16**, the most effective and the least effective CA II inhibitor in this series, whose only difference consists in the positions of the two methyl groups substituting the aniline functionality in ortho to the sulfamoyl group. These data are in agreement with previously reported studies on other sulfonamides/sulfamates/sulfamides possessing CA inhibitory properties and have been explained at the molecular level by reporting the X-ray crystal structures of such adducts with CA II.[16–18] These structures evidencing clashes between certain moieties of the inhibitor and amino acid residues within the enzyme active site (in addition to favorable interactions that allow the complexation of the inhibitor within the cavity) can explain why even a minor structural difference between two compounds, e.g., an additional CH_2 moiety, may lead to very different inhibitory effects against various CA isozymes.[16–18]

Finally, it is also worth noting the finding that amine **2** is in this case a much more effective inhibitor as compared to the corresponding nitro-derivative **1**, proving that the pK_a alone is not a sufficiently important factor to influence the inhibitory capacity (as stressed above, just the reverse situation was true for the inhibition of isoform CA I, against which **1** was a much stronger inhibitor than **2**).

Against the tumor-associated isoform CA IX, the sulfonamides investigated here showed a very interesting inhibitory activity. Thus, three compounds, **A6**, **A16**, and **B3**, were moderate inhibitors, with K_Is in the range of 93−289 nM, whereas the other five derivatives were slightly better inhibitors (i.e., **1**, **2**, **A5**, **A12**, and **A15** showing K_Is in the range of 33.4−85 nM, Table 1). However, compounds **A1**−**A4**, **A7**−**A11**, **A13**, **A14**, **A17**−**A20**, and **B1**, **B2** behaved as very potent CA IX inhibitors, with K_Is in the range of 7.4−14 nM, being generally more effective than the clinically used derivatives **AZA**−**IND**. Again, SAR is rather flat for this series of compounds, as discussed above for CA I and II. In fact, the best inhibitors incorporate both aliphatic as well as aromatic, secondary, or tertiary amine moieties in ortho to the sulfamoyl group. As for CA II, the amino derivative **2** was almost a two times more effective CA IX inhibitor as compared to the corresponding nitroderivative **1**, which for a potentially bioreducible compound is an important observation (Table 1).

CA XII was well inhibited by most derivatives investigated here, similarly to CA IX. In fact, we have shown earlier[23] that CA XII is a sulfonamide-avid isoform, being strongly inhibited by many types of sulfonamides, including the clinically used derivatives **AZA**−**IND**[23] (see also Table 1). Thus, only **A6** and **A16** were weaker CA XII inhibitors (K_Is of 175−246 nM), all other compounds showing a very potent inhibitory activity, with K_Is in the range of 5.8−79 nM.

The findings reported here show that many of the sulfonamides investigated here act as CA IX/XII selective inhibitors, possessing a higher affinity for the tumor-associated over the cytosolic isozymes CA I and II (Table 2). Generally, the selectivity ratio toward CA I is not a problem because this isozyme is known to have a lower affinity for sulfonamide CAIs, as compared to CA II, due to the presence of several bulky amino acid residues (such as His200 and His67 among others) within the active site.[1,2,18] Indeed, the selectivity ratios for the inhibition of both hCA IX and hCA XII over hCA I are very good, in the ranges of 162.3−1391 (hCA I/hCA IX), and 11.7−1395 (hCA I/hCA XII), respectively (Table 2). However, the inhibition profiles of CA II and IX (or CA II and XII) are generally much more similar. It is difficult to obtain compounds with a better affinity for the tumor-associated isozymes over CA II (for example, all the clinically used inhibitors have selectivity ratios for the inhibition of CA II over CA IX < 1, see Table 2).[1–3] Data of Table 2 show that the nitro-sulfonamides investigated here are better CA IX inhibitors than CA II inhibitors, with selectivity ratios in the range of 1.54−12.4. The selectivity ratios for the inhibition of CA XII over CA II are even higher, being in the range of 4.27−16.9. These data clearly demonstrate that the class of sulfonamides investigated here shows some significant levels of selectivity for the inhibition of the tumor-associated isozymes CA IX and XII over the cytosolic, house-keeping isozymes CA I and II. This is indeed a very important result, which can be used to find a rationale in the drug design of selective CA inhibitors. In the literature, a series of amino acids located in the active site was reported to be involved in inhibitor recognition and to have a role in the selectivity of various inhibitors toward different isozymes.[6,17,20–22] In particular, the amino acid in position 131, which is Phe for hCA II, Leu for hCA I, Val for hCA IX, and Ala for hCA XII (see Figure 1),[1–3] is known to be very important for the binding of sulfonamide inhibitors to CAs.[6] As an example, in the case of hCA II, the bulky side chain of this Phe residue limits the space available for the inhibitors, or it may participate in stacking interactions with aromatic groups. The presence of a less bulky such residue in hCA IX (i.e., a valine) has as a consequence the fact that the hCA IX active site is larger than that of hCA II and can accommodate bulkier inhibitors. (for recent examples, see refs 20, 21). The presence of a less bulky such residue in hCA IX (i.e., a valine), which is also unavailable for participation to stacking interactions, has as a consequence the fact that the hCA IX active site is larger than that of hCA II. A second residue that drew our attention is 132, which is Gly in hCA II, Ala in hCA I, Asp in hCA IX, and Ser in hCA XII (Figure 1). This residue is situated on the rim of the active site cavity of hCA II (and presumably also of hCA IX, for which the X-ray crystal structure has not yet been reported)[1–3] and it is critical for the interaction with inhibitors possessing elongated molecules, as recently shown by our group.[22] Strong hydrogen bonds involving the CONH moiety of Gly132 were shown to stabilize the complex of this isozyme with a *p*-aminoethylbenzenesulfonamide derived inhibitor.[22] In the case of hCA IX, the presence of aspartic acid in this position at the entrance of the active site may signify that: (i) stronger interactions with polar moieties of the inhibitor should be possible, (ii) this residue may have flexible conformations, fine-tuning in this way the interaction with inhibitors. Finally, the residue in position 65, which is Ala for hCA II and Ser for hCA I, hCA IX ,and hCA

Table 2. Selectivity Ratios for the Inhibition of the Tumor-Associated (CA IX and XII) over the Cytosolic (CA I and II) Isozymes with Selected CAIs Reported Here

	selectivity ratio			
compound	hCA I/hCA IX	hCA II/hCA IX	hCA I/hCA XII	hCA II/hCA XII
AZA	10.0	0.48	43.8	2.10
MZA	1.85	0.51	14.7	4.11
EZA	0.73	0.23	1.13	0.36
1	2.8	2.77	11.7	11.6
2	162.3	1.54	590.5	5.60
A2	1104	10.6	943	9.10
A4	1323	8.33	1395	8.79
A11	450	7.14	547	8.69
A17	1391	6.81	872	4.27
A20	455	12.4	620	16.9
B1	280	4.00	336	4.81

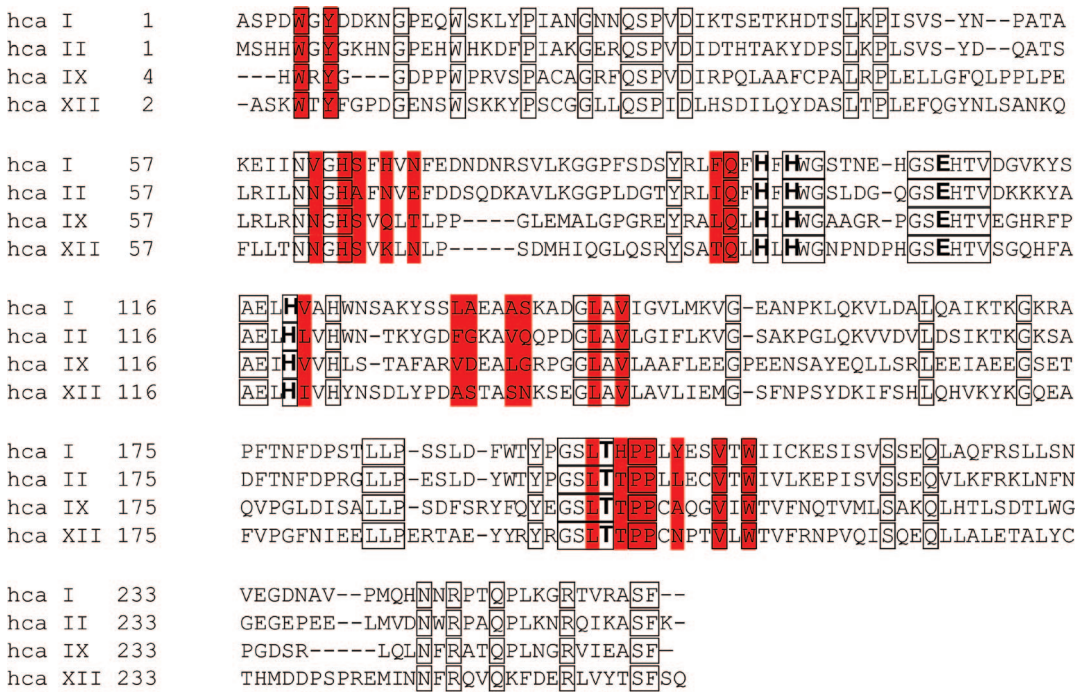

Figure 1. Sequence alignment of hCA I, hCA II, hCA IX, and hCA XII. Highly conserved residues are boxed, catalytic histidines, Thr199 and Glu106 are in bold, while residues delimiting the active site cavity are highlighted in red.

XII, has also been reported to have an important role in discriminating inhibitor binding affinity toward different isozymes.[17]

Because a careful comparison between the amino acid sequences of the isozymes I, II, IX, and XII reveals several other important amino acid substitutions within their active sites (see Figure 1), we have undertaken a crystallographic and molecular modeling study to identify which residues could be responsible for the selectivity properties toward the different CA isozymes of the class of molecules here investigated.

X-Ray Crystallography. The structure of the isozyme hCA II with the lead compound **1** has been solved. In particular, this compound was chosen because it presents a 2-substituted-5-nitrobenzenesulfonamide scaffold that is common to all the other molecules investigated here; thus structural determinants responsible of its binding properties can be easily extended to all other members of this inhibitor family.

The hCA II−**1** complex was prepared and crystallized using experimental conditions previously reported for other sulfonamide CA inhibitors and the structure was solved using the difference Fourier method, with the structure of the native hCA II as starting model.[24] The crystallographic *R*-factor and *R*-free, calculated in the 20.00−1.45 Å resolution range, were 0.192 and 0.207, respectively; the statistics for data collection and refinement are shown in Table 3.

Analysis of the electron density maps of the hCA II−**1** complex clearly showed the presence of one inhibitor molecule in the enzyme catalytic site, with an entirely defined electron density (Figure 2). The topology of the inhibitor binding within the active site is shown in Figure 3. In particular, the sulfonamide group of **1** was coordinated to the Zn(II) ion within the hCA II cavity, with other residues participating to the stabilization of the E−I complex, similarly to what observed for the same moiety in other inhibitors for which the structure has been solved in complex with the enzyme (Figure 3).[5−7,16−22] Moreover, the phenyl ring of **1** established strong Van der Waals contacts with residues Gln92, His94, Val121, Phe131, Leu198, and Thr200. Its chlorine atom also interacted with the aliphatic side chain of various hydrophobic residues (Val121, Leu141, Val 143, Leu198, and Val207). The NO_2 group of the inhibitor, whose plane was oriented perpendicularly to that of the phenyl ring, was directed toward the hydrophilic side of the active site cleft, establishing hydrogen bonds with residues His64 and Thr200 and with two water molecules (Figure 3). Around this NO_2 group, a weak electron density was observed that seemed to suggest the presence of a second conformation for this moiety,

Table 3. Crystal Parameters, Data Collection and Refinement Statistics for the hCA II−**1** Complex[a]

crystal parameters	
space group	$P2_1$
a (Å)	42.07
b (Å)	41.24
c (Å)	71.83
β (deg)	104.20
data collection statistics	
resolution (Å)	(20.00−1.45)
wavelength (Å)	1.200
temperature (K)	100
total reflections	118328
unique reflections	41454
completeness (%)	97.3 (77.2)
R-sym[b] (%)	4.5 (21.1)
mean $I/\sigma(I)$	18.6 (4.1)
refinement statistics	
R-factor[c](%)	19.2
R-free[c]rmsd(%)	20.7
bond lengths (Å)	0.005
bond angles (deg)	1.4
number of protein atoms	2101
number of inhibitor atoms	14
number of water molecules	358
average B factor (Å^2)	13.71

[a] Values in parentheses refer to the highest resolution shell. [b] *R*-sym = $\sum|I_i - \langle I\rangle|/\sum I_i$ over all reflections. [c] *R*-factor = $\sum|F_o - F_c|\sum/F_o$; *R*-free calculated with 5% of data withheld from refinement.

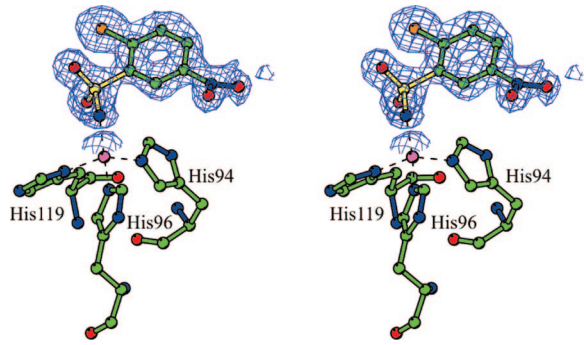

Figure 2. Stereo view of the active site region in the hCAII−**1** complex. The simulated annealing omit $2F_o - F_c$ electron density map relative to the inhibitor molecule is shown. The active site Zn^{2+} ion coordination is also reported (dotted lines).

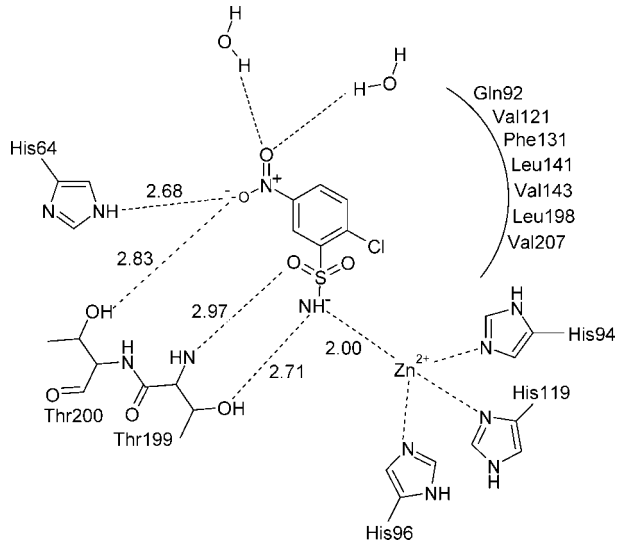

Figure 3. Active site region in the hCA II−**1** complex X-ray structure, showing residues participating in recognition of the inhibitor molecule.

whose plane was planar with respect to that of the phenyl ring (data not shown).

A careful analysis of the hCA II−**1** complex structure revealed that the phenyl ring of the inhibitor was oriented in the enzyme active site differently from that observed in other hCA II−benzenesulfonamides complexes (Figure 4).[19] Thus, the plane of the phenyl ring appeared rotated by almost 45° and tilted by approximately 10° with respect to the canonical orientation[5–7] as a result of the interaction of the NO_2 group with Thr200 and His64 (Figure 4). Recently, this conformation was also observed for benzene-1,3-disulfonamides containing derivatives, such as **DCP**,[19] being ascribed, also in this case, to the presence of a rather bulky meta-substitutent relative to the sulfamoyl zinc-binding function within the inhibitor molecule, able to establish polar interactions with hCA II residues delimiting the hydrophilic part of the active site (Figure 4).

Modeling Studies and Molecular Dynamics Simulations. To identify the molecular features responsible for the differences observed in the affinity of **1** toward hCA II and hCA IX (Table 1), a model of the hCA IX−**1** complex was built up by homology modeling and molecular dynamics simulation approaches. The main protein−inhibitor interactions evidenced using this procedure are schematically depicted in Figure 5. A comparison of this model with the crystallographic structure of the hCA II−**1** complex revealed important differences in the

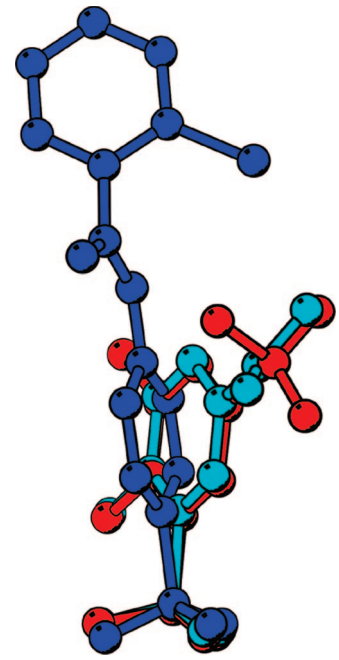

Figure 4. Superposition of inhibitors **1** (colored in cyan), **DCP** (colored in red), and **4** (colored in blue) when bound within the CA II active site.

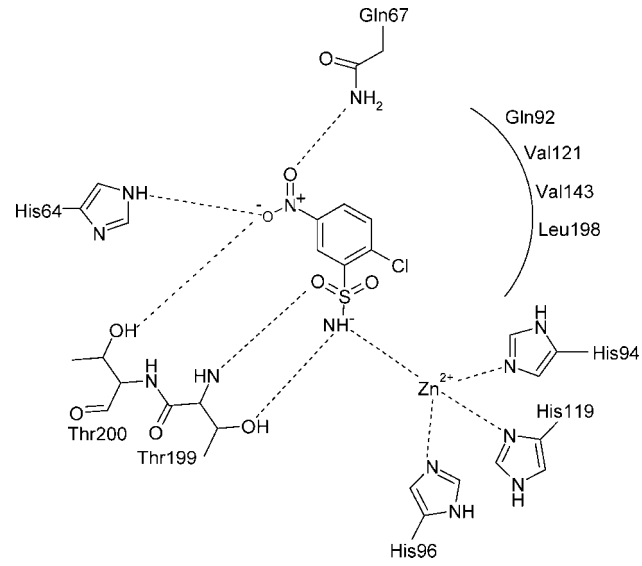

Figure 5. Model of the hCA IX−**1** adduct from MD simulations. Residues participating in recognition of the inhibitor molecule are reported.

binding mode of this inhibitor to the two isoforms. In particular, whereas the tetrahedral geometry of the Zn^{2+} binding site and the key hydrogen bonds between the sulfonamide moiety of the inhibitor and enzyme active site were all retained in both complexes, the pattern of hydrogen bonds involving the hCA IX enzyme and the oxygens of inhibitor NO_2 group, even if conserved with respect to hCA II−**1** complex, was enriched by an additional interaction. Thus, Asn67 present in the hCA II active site is replaced in hCA IX by Gln67, which, as a consequence of its longer side chain, is able to form a stable hydrogen bond with the inhibitor NO_2 oxygen atoms. In addition, the interaction of His64 with the inhibitor is further optimized by the formation of another hydrogen bond between its ND2 atom and the hydroxyl group of Ser65, which in hCA IX replaces Ala65 present in hCA II. In conclusion, a rather

different pattern of polar interactions within the enzyme active site, caused by specific amino acid substitutions, might explain the 2.77-fold higher inhibition efficiency of compound **1** toward hCA IX with respect to hCA II.

Conclusions

A large series of 2-substituted-5-nitro-benzenesulfonamides, incorporating a large variety of secondary/tertiary amines in ortho to the sulfamoyl moiety, were explored as inhibitors of several physiologically/pathologically relevant CA isozymes with the aim of designing bioreducible inhibitors targeting the hypoxia overexpressed, tumor-associated isozymes CA IX/XII. The investigated compounds were ineffective inhibitors of the cytosolic isoform CA I (in the micromolar range), showed a better inhibition of the physiologically relevant, house-keeping isoform CA II (K_Is of 8.8−4975 nM), but strongly inhibited the tumor-associated CA IX and XII (K_Is of 7.4−653 nM against CA IX, and 5.8−175 nM against CA XII, respectively). Some of these compounds showed excellent selectivity ratios (in the range of 10−1395) for the inhibition of the tumor associated over the cytosolic isozymes. The X-ray crystal structure of the adduct of hCA II with the lead molecule 2-chloro-5-nitro-benzenesulfonamide as well as molecular modeling studies for its interaction with hCA IX afforded a better understanding of the factors governing the discrimination of the two isoforms for this type of bioreductive compounds targeting specifically hypoxic tumors.

Experimental Section

The hCA II−**1** complex was obtained by adding a 3-molar excess of inhibitors to a 10 mg/mL protein solution in 100 mM Tris-HCl pH 8.5. Crystals of the complex were obtained using the hanging drop vapor diffusion technique. In particular, 2 μL of complex solution were mixed with 2 μL of precipitant solution (2.5 M $(NH_4)_2SO_4$, 0.3 M NaCl, 100 mM Tris-HCl (pH 8.2), and 5 mM 4-(hydroxymercurybenzoic) acid) and suspended over a reservoir containing 1 mL of precipitant solution at 22 °C. Crystals grew within a few days and were isomorphous to those of the native enzyme.[24] X-ray diffraction data were collected at 100 K, at the Synchrotron source Elettra in Trieste, using a Mar CCD detector. Prior to cryogenic freezing, the crystals were transferred to the precipitant solution with the addition of 15% (v/v) glycerol. Diffracted data were processed using the HKL crystallographic data reduction package.[25] Diffraction data were indexed in the $P2_1$ space group with one molecule in the asymmetric unit. Unit cell parameters and data reduction statistics are summarized in Table 3. The enzyme−inhibitor complex structure was analyzed by difference Fourier techniques, using the atomic coordinates of the native hCA II (PDB entry 1CA2)[24] as starting model. The refinement was carried out with the program CNS,[26] whereas the model building and map inspections were performed using the O program.[27] Fourier maps calculated with $|3F_o - 2F_c|$ and $|F_o - F_c|$ coefficients showed prominent electron density features in the active site region. After initial refinement limited to the enzyme, the inhibitor molecule was gradually built into the model for further refinement. Restraints on inhibitor bond angles and distances were taken from similar structures in the Cambridge Structural Database, and standard restraints were used on protein bond angles and distances throughout refinement. The ordered water molecules were added automatically and checked individually. Each peak contoured at 3σ in the $|F_o - F_c|$ maps was identified as a water molecule, provided that hydrogen bonds would be allowed between this site and the model. The correctness of stereochemistry was finally checked using PROCHECK.[28] Final refinement statistics are reported in Table 3. Coordinates and structure factors have been deposited with the Protein Data Bank (accession code 2QP6).

Modeling Studies and Molecular Dynamics Simulations. A model of the hCA IX catalytic domain (G12-F260) was built as previously reported by Alterio et al.[5] Briefly, the sequence of hCA IX was retrieved from publicly available sequence database Swiss-Prot/TrEMBL (primary accession number Q16790)[29] and was modeled using both hCA II (34% sequence identity) and hCA XIV (34% sequence identity) (PDB entry 1RJ6)[30] X-ray structures as templates. Fifty homology models were built with MODELER version 6.2,[31] and their quality was assessed by using PROCHECK[28] and 3D-profile module[32] of INSIGHT II (Accelrys Software Inc.). The best model in term of PROCHECK G-factor and 3D-profile score was then complexed to the inhibitor by superimposing the heavy atoms from the three Zn^{2+} coordination histidines of hCA II−**1** structure to corresponding atoms of hCA IX model. The hCA IX−**1** complex was completed by addition of all hydrogen atoms and underwent energy minimization with the SANDER module of AMBER9 package[33] using the PARM99 force field.[34] Atomic charges of **1** were obtained with the RESP methodology.[35] The conformation of **1** derived from the hCA II−**1** crystal structure was fully optimized using the GAMESS program[36] at the Hartree−Fock level with STO-3G basis set. Single-point calculations on optimized molecule were performed at the RHF/6-31G* level. The resulting electrostatic potential was thus used for a one-stage single-conformation RESP charge fitting. Partial charges for the three histidines and the zinc ion were those published by Suarez and Merz.[37] To preserve the integral charge of the whole system, partial charges of Cα and Hα atoms of the zinc−ligand residues and of the N and H atoms belonging to the inhibitor sulfonamide group were modified accordingly. A bonded approach between Zn^{2+} ion and its ligands ensured the experimentally observed tetrahedral Zn^{2+} coordination in all complexes during the MD simulations. Equilibrium bond distances and angles were taken from the hCA II crystal structure.[24] Force constant values of 120, 20, and 30 kcal mol^{-1} Å^{-1} were used for N(His)−Zn, N(His)−Zn−N(His) and N(His)−Zn−N(sulfonamide) bond stretching and angle bending parameters, respectively. All the torsional parameters associated with Zn−ligand interactions were set to zero according to Hoops et al.[38]

To perform the MD simulation in the presence of solvent, the minimized complexes were confined in truncated octahedron boxes (x, y, z = 80 Å) filled with TIP3P water molecules and counterions (Na^+) to neutralize the system. The solvated molecules were then energy minimized through 1000 steps with solute atoms restrained to their starting positions by using a force constant of 10 kcal mol^{-1} Å^{-1} prior to the MD simulations. After this, the molecules were submitted to 90 ps restrained MD (5 kcal mol^{-1} Å^{-1}) at constant volume, gradually heating to 300 K, followed by 60 ps restrained MD (5 kcal mol^{-1} Å^{-1}) at constant pressure to adjust the system density. Production MD simulations were carried out at 300 K and a constant pressure for 1 ns with a time-step of 1.5 fs. Bonds involving hydrogens were constrained using the SHAKE algorithm.[39] Snapshots from production run were saved every 1000 steps and analyzed with MOLMOL program.[40]

Acknowledgment. We thank the Sincrotrone Trieste C.N.R./Elettra, for giving us the opportunity to collect data at the Crystallographic Beamline. This research was financed in part by two grants of the 6th Framework Programme of the European Union (EUROXY and DeZnIT projects).

References

(1) Supuran, C. T. Carbonic anhydrases: novel therapeutic applications for inhibitors and activators. *Nat. Rev. Drug Discovery* **2008**, *7*, 168–181.

(2) Supuran, C. T.; Scozzafava, A. Carbonic anhydrases as targets for medicinal chemistry. *Bioorg. Med. Chem.* **2007**, *15*, 4336–4350.

(3) Thiry, A.; Dogné, J. M.; Masereel, B.; Supuran, C. T. Targeting tumor-associated carbonic anhydrase IX in cancer therapy. *Trends Pharmacol. Sci.* **2006**, *27*, 566–573.

(4) Pastorekova, S.; Kopacek, J.; Pastorek, J. Carbonic Anhydrase Inhibitors and the Management of Cancer. *Curr. Top. Med. Chem.* **2007**, *7*, 865–878.

(5) Alterio, V.; Vitale, R. M.; Monti, S. M.; Pedone, C.; Scozzafava, A.; Cecchi, A.; De Simone, G.; Supuran, C. T. Carbonic Anhydrase Inhibitors: X-ray and Molecular Modeling Study for the Interaction of a Fluorescent Antitumor Sulfonamide with Isozyme II and IX. *J. Am. Chem. Soc.* **2006**, *128*, 8329–8335.
(6) Menchise, V.; De Simone, G.; Alterio, V.; Di Fiore, A.; Pedone, C.; Scozzafava, A.; Supuran, C. T. Carbonic Anhydrase Inhibitors: Stacking with Phe131 Determines Active Site Binding Region of Inhibitors As Exemplified by the X-ray Crystal Structure of a Membrane-Impermeant Antitumor Sulfonamide Complexed with Isozyme II. *J. Med. Chem.* **2005**, *48*, 5721–5727.
(7) De Simone, G.; Vitale, R. M.; Di Fiore, A.; Pedone, C.; Scozzafava, A.; Montero, J. L.; Winum, J. Y.; Supuran, C. T. Carbonic Anhydrase Inhibitors: Hypoxia-Activatable Sulfonamides Incorporating Disulfide Bonds that Target the Tumor-Associated Isoform IX. *J. Med. Chem.* **2006**, *49*, 5544–5551.
(8) Raether, W.; Hane, H. Nitroheterocyclic drugs with broad spectrum activity. *Parasitol. Res.* **2003**, *90*, S19–S39.
(9) Anderson, R. F.; Shinde, S. S.; Hay, M. P.; Denny, W. A. Potentiation of the cytotoxicity of the anticancer agent tirapazamine by benzotriazine *N*-oxides: The role of redox equilibra. *J. Am. Chem. Soc.* **2006**, *128*, 245–249.
(10) Ljungkvist, A. S.; Bussink, J.; Kaanders, J. H.; van der Kogel, A. J. Dynamics of tumor hypoxia measured with bioreductive hypoxic cell markers. *Radiat. Res.* **2007**, *167*, 127–145.
(11) Nutt, R.; Vento, L. J.; Ridinger, M. H. T. In Vivo Molecular Imaging Biomarkers: Clinical Pharmacology's new "PET". *Clin. Pharmacol. Ther.* **2007**, *81*, 792–795.
(12) Arteel, G. E.; Raleigh, J. A.; Bradford, B. U.; Thurman, R. G. Acute alcohol produces hypoxia directly in rat liver tissue in vivo: role of Kupffer cells. *Am. J. Physiol.* **1996**, *271*, G494–G500.
(13) Mallia, M. B.; Mathur, A.; Subramanian, S.; Banerjee, S.; Sarma, H. D.; Venkatesh, M. A novel $[^{99m}Tc{\equiv}N]^{2+}$ complex of metronidazole xanthate as a potential agent for targeting hypoxia. *Bioorg. Med. Chem. Lett.* **2005**, *15*, 3398–3401.
(14) Hanson, J.; Dogné, J. M.; Ghiotto, J.; Moray, A. L.; Kinsella, B. T.; Pirotte, B. Design, synthesis, and SAR study of a series of *N*-alkyl-*N*′-[2-(aryloxy)-5-nitrobenzenesulfonyl]ureas and -cyanoguanidine as selective antagonists of the TPalpha and TPbeta isoforms of the human thromboxane A2 receptor. *J. Med. Chem.* **2007**, *50*, 3928–3936.
(15) Khalifah, R. G. The carbon dioxide hydration activity of carbonic anhydrase I. Stop-flow kinetic studies on the native human isoenzymes B and C. *J. Biol. Chem.* **1971**, *246*, 2561–2573.
(16) Casini, A.; Antel, J.; Abbate, F.; Scozzafava, A.; David, S.; Waldeck, H.; Schäfer, S.; Supuran, C. T. Carbonic anhydrase inhibitors: SAR and X-ray crystallographic study for the interaction of sugar sulfamates/sulfamides with isozymes I, II, and IV. *Bioorg. Med. Chem. Lett.* **2003**, *13*, 841–845.
(17) Winum, J. Y.; Temperini, C.; El Cheikh, K.; Innocenti, A.; Vullo, D.; Ciattini, S.; Montero, J. L.; Scozzafava, A.; Supuran, C. T. Carbonic anhydrase inhibitors: clash with Ala65 as a means for designing inhibitors with low affinity for the ubiquitous isozyme II, exemplified by the crystal structure of the topiramate sulfamide analogue. *J. Med. Chem.* **2006**, *49*, 7024–7031.
(18) Temperini, C.; Innocenti, A.; Guerri, A.; Scozzafava, A.; Rusconi, S.; Supuran, C. T. Phosph(on)ate as a zinc-binding group in metalloenzyme inhibitors: X-ray crystal structure of the antiviral drug foscarnet complexed to human carbonic anhydrase I. *Bioorg. Med. Chem. Lett.* **2007**, *17*, 2210–2215.
(19) Alterio, V.; De Simone, G.; Monti, S. M.; Scozzafava, A.; Supuran, C. T. Carbonic anhydrase inhibitors: inhibition of human, bacterial, and archaeal isozymes with benzene-1,3-disulfonamides: solution and crystallographic studies. *Bioorg. Med. Chem. Lett.* **2007**, *17*, 4201–4207.
(20) Güzel, Ö.; Temperini, C.; Innocenti, A.; Scozzafava, A.; Salman, A.; Supuran, C. T. Carbonic anhydrase inhibitors. Interaction of 2-(hydrazinocarbonyl)-3-phenyl-1*H*-indole-5-sulfonamide with 12 mammalian isoforms: kinetic and X-ray crystallographic studies. *Bioorg. Med. Chem. Lett.* **2008**, *18*, 152–158.
(21) Di Fiore, A.; Pedone, C.; D'Ambrosio, K.; Scozzafava, A.; De Simone, G.; Supuran, C. T. Carbonic anhydrase inhibitors: Valdecoxib binds to a different active site region of the human isoform II as compared to the structurally related cyclooxygenase II "selective" inhibitor celecoxib. *Bioorg. Med. Chem. Lett.* **2006**, *16*, 437–442.
(22) Casini, A.; Abbate, F.; Scozzafava, A.; Supuran, C. T. Carbonic anhydrase inhibitors: X-ray crystallographic structure of the adduct of human isozyme II with a bis-sulfonamide: two heads are better than one. *Bioorg. Med. Chem. Lett.* **2003**, *13*, 2759–2763.
(23) Vullo, D.; Innocenti, A.; Nishimori, I.; Pastorek, J.; Scozzafava, A.; Pastorekova, S.; Supuran, C. T. Carbonic anhydrase inhibitors. Inhibition of the transmembrane isozyme XII with sulfonamides: a new target for the design of antitumor and antiglaucoma drugs. *Bioorg. Med. Chem. Lett.* **2005**, *15*, 963–969.
(24) Eriksson, A. E.; Jones, T. A.; Liljas, A. Refined structure of human carbonic anhydrase II at 2.0 Å resolution. *Proteins: Struct., Funct.* **1988**, *4*, 274–282.
(25) Otwinowski, Z.; Minor, W. Processing of X-ray Diffraction Data Collected in Oscillation Mode. *Methods Enzymol.* **1997**, *276*, 307–326.
(26) Brünger, A. T.; Adams, P. D.; Clore, G. M.; De Lano, W. L.; Gros, P.; Grosse-Kunstleve, R. W.; Jiang, J. S.; Kuszewski, J.; Nilges, M.; Pannu, N. S.; Read, R. J.; Rice, L. M.; Simonson, T.; Warren, G. L. Crystallography & NMR system: A new software suite for macromolecular structure determination. *Acta Crystallogr., Sect. D: Biol Crystallogr.* **1998**, *54*, 905–921.
(27) Jones, T. A.; Zou, J. Y.; Cowan, S. W.; Kjeldgaard, M. Improved methods for building protein models in electron density maps and the location of errors in these models. *Acta Crystallogr., Sect. A: Found. Crystallogr.* **1991**, *47*, 110–119.
(28) Laskowski, R. A.; MacArthur, M. W.; Moss, D. S.; Thornton, J. M. PROCHECK: a program to check the stereochemical quality of protein structures. *J. Appl. Crystallogr.* **1993**, *26*, 283–291.
(29) Boeckmann, B.; Bairoch, A.; Apweiler, R.; Blatter, M. C.; Estreicher, A.; Gasteiger, E.; Martin, M. J.; Michoud, K.; O'Donovan, C.; Phan, I.; Pilbout, S.; Schneider, M. The SWISS-PROT protein knowledgebase and its supplement TrEMBL in 2003. *Nucleic Acids Res.* **2003**, *31*, 365–370.
(30) Whittington, D. A.; Grubb, J. H.; Waheed, A.; Shah, G. N.; Sly, W. S.; Christianson, D. W. Expression, assay, and structure of the extracellular domain of murine carbonic anhydrase XIV: implications for selective inhibition of membrane-associated isozymes. *J. Biol. Chem.* **2004**, *279*, 7223–7228.
(31) Sali, A.; Blundell, T. L. Comparative protein modelling by satisfaction of spatial restraints. *J. Mol. Biol.* **1993**, *234*, 779–815.
(32) Bowie, J. U.; Luthy, R.; Eisenberg, D. A method to identify protein sequences that fold into a known three-dimensional structure. *Science* **1991**, *253*, 164–170.
(33) Case, D. A.; Darden, T. A.; Cheatham, T. E., III; Simmerling, C. L.; Wang, J.; Duke, R. E.; Luo, R.; Merz, K. M.; Pearlman, D. A.; Crowley, M.; Walker, R. C.; Zhang, W.; Wang, B.; Hayik, S.; Roitberg, A.; Seabra, G.; Wong, K. F.; Paesani, F.; Wu, X.; Brozell, S.; Tsui, V.; Gohlke, H.; Yang, L.; Tan, C.; Mongan, J.; Hornak, V.; Cui, G.; Beroza, P.; Mathews, D. H.;. Schafmeister, C.; Ross, W. S.; Kollman, P. A. *AMBER 9*; University of California: San Francisco, 2006.
(34) Wang, J.; Cieplak, P.; Kollman, P. A. How Well Does a RESP (Restrained Electrostatic Potential) Model Do in Calculating the Conformational Energies of Organic and Biological Molecules? *J. Comput. Chem.* **2000**, *21*, 1049–1074.
(35) Bayly, C. I.; Cieplak, P.; Cornell, W.; Kollman, P. A. A well-behaved electrostatic potential based method using charge restraints for deriving atomic charges: the RESP model. *J. Phys. Chem.* **1993**, *97*, 10269–10280.
(36) Schmidt, M. W.; Baldridge, K. K.; Boatz, J. A.; Elbert, S. T.; Gordon, M. S.; Jensen, J. J.; Koseki, S.; Matsunaga, N.; Nguyen, K. A.; Su, S.; Windus, T. L.; Dupuis, M.; Montgomery, J. A. General Atomic and Molecular Electronic Structure System. *J. Comput. Chem.* **1993**, *14*, 1347–1363.
(37) Suarez, D.; Merz, K. M. Molecular Dynamics Simulations of the Mononuclear Zinc-β-lactamase from *Bacillus cereus*. *J. Am. Chem. Soc.* **2001**, *123*, 3759–3770.
(38) Hoops, S. C.; Anderson, K. W.; Merz, K. M. Force field design for metalloproteins. *J. Am. Chem. Soc.* **1991**, *113*, 8262–8270.
(39) Ryckaert, J.-P.; Ciccotti, G.; Berendsen, H. J. C. Numerical integration of the cartesian equations of motion of a system with constraints: molecular dynamics of *n*-alkanes. *J. Comput. Phys.* **1977**, *23*, 327–341.
(40) Koradi, R.; Billeter, M.; Wuthrich, K. MOLMOL: a program for display and analysis of macromolecular structures. *J. Mol. Graphics* **1996**, *14*, 51–55.

JM800121C